3. T. L. Morkved, P. Wiltzius, H. M. Jaeger, D. G. Grier, T. A. Witten, *Appl. Phys. Lett.* **64**, 422 (1994); R. Saito, S. Okamura, K. Ishizu, *Polymer* **33**, 1099 (1992); K. Ishizu *et al.*, *ibid.* **34**, 2256 (1993); R. S. Saunders, R. E. Cohen, R. R. Schrock, *Macromolecules* **24**, 5599 (1991); Y. Ng, C. Chan, R. R. Schrock, R. E. Cohen, *Chem. Mater.* **4**, 24 (1992); R. Tassoni and R. R. Schrock, *ibid.* **6**, 744 (1994).
4. J. P. Spatz, A. Roescher, S. Sheiko, G. Krausch, M. Moller, *Adv. Mater.* **7**, 731 (1995).
5. P. Mansky, P. Chaikin, E. L. Thomas, *J. Mater. Sci.* **30**, 1987 (1995); *Appl. Phys. Lett.* **68**, 2586 (1996).
6. E. L. Thomas, D. J. Kinning, D. B. Alward, C. S. Henkee, *Macromolecules* **20**, 2934 (1987).
7. Y. Liu *et al.*, *ibid.* **27**, 4000 (1994).
8. A. Keller, E. Pedemonte, F. M. Willmouth, *Nature* **225**, 538 (1970); G. Hadziiannou, A. Mathis, A. Skoulious, *Colloid Polym. Sci.* **257**, 136 (1979); K. A. Koppi, M. Tirrell, F. S. Bates, K. Almdal, R. H. Colby, *J. Phys. (Paris)* **2**, 1941 (1993).
9. K. Amundson *et al.*, *Macromolecules* **24**, 6546 (1991); K. Amundson, E. Helfand, X. Quan, S. D. Hudson, S. D. Smith, *ibid.* **27**, 6559 (1994).
10. K. Amundson, E. Helfand, X. Quan, S. D. Smith, *ibid.* **26**, 2698 (1993).
11. For related work on polymer blends, see G. Venugopal, S. Krause, G. Wnek, *Chem. Mater.* **4**, 1334 (1992); J. M. Serpico *et al.*, *Macromolecules* **25**, 6373 (1992).
12. Our substrates consisted of a 100-nm-thick silicon nitride layer deposited onto a silicon wafer. The silicon was selectively etched away from the backside of the wafer under small rectangular areas, providing self-supporting, transparent silicon nitride membranes with lateral dimensions of 60 μm. We fabricated planar electrodes with gap spacings of 4 μm on top of the silicon nitride within the window areas using optical or electron-beam lithography followed by evaporation of 25-nm chromium. Small gold wires were attached with silver epoxy and connected to a programmable voltage source.
13. At this temperature, the product of Flory-Huggins interaction parameter, χ, and number of monomers per chain, N, for our polymers is $\chi N \sim 30$, putting us in the strong segregation limit. See T. P. Russell, R. P. Hjelm, P. A. Seeger, *Macromolecules* **23**, 890 (1990); T. P. Russell, *ibid.* **26**, 5819 (1993).
14. T. L. Morkved *et al.*, in preparation.
15. C. S. Henkee, E. L. Thomas, L. J. Fetters, *J. Mater. Sci.* **23**, 1685 (1988).
16. E. L. Thomas and Y. Talmon, *Polymer* **19**, 225 (1978).
17. To minimize systematic errors that arise from the finite resolution of any digital image processing routine, we consider a normalized order parameter S, defined as $S(E) = [C(E) - C_{min}]/(C_{max} - C_{min})$. Here $C(E) = 2\langle\cos^2\theta\rangle - 1$; C_{max} and C_{min} are the order parameters obtained by image processing from a perfectly aligned region containing no defects and from an unaligned sample annealed without an applied E field, respectively.
18. E. V. Gurovich [*Macromolecules* **27**, 7063 (1994)] proposed that alignment in copolymers is due to field-induced changes in the coil conformations. Because the anisotropic part of the polarizability of most monomers is much smaller than the average polarizability, this mechanism can be neglected for nonpolar systems compared to the effect treated by Amundson *et al.* [see A. Onuki and J. Fukuda, *Macromolecules* **28**, 8788 (1995)]. Even though PMMA does contain permanent dipoles, we can estimate their contribution and find it not significant [see also the discussion in (*10*)].
19. R. F. Boyer, in *Encyclopedia of Polymer Science and Technology* (Intersciences, New York, 1970), vol. 13, pp. 251–277; N. G. McCrum, B. E. Read, G. Williams, *Anelastic and Dielectric Effects in Polymeric Solids* (Wiley, New York, 1967), p. 264.
20. $\Delta F = (\gamma/8\pi)(\Delta\varepsilon E)^2/\langle\varepsilon\rangle$, in centimeter-gram-second units, where the coefficient γ depends on the details of the domain geometry. In the case of cylindrical domains, as in our samples, $\gamma = 1/9$.
21. K. Amundson and E. Helfand, *Macromolecules* **26**, 1324 (1993).
22. Systematic studies of the effect of changing the annealing conditions are in progress. The degree of alignment in E fields <30 kV/cm might improve with different annealing conditions, leading to a reduction in the saturation field for the order parameter $S(E)$. However, improvements in the ordering of unaligned samples under the same conditions are also likely, leading to an increase in the average radius of curvature and a decrease in the curvature energy.
23. We thank T. A. Witten, F. J. Solis, and S. R. Nagel for helpful discussions. Supported in part by the Medical Research Science and Engineering Center program of the National Science Foundation (NSF) under award DMR-9400379. The silicon nitride membranes were fabricated at the National Nanofabrication Facility at Cornell University, which is supported by the National Science Foundation under grant ECS-8619049. H.M.J. acknowledges fellowship support from the David and Lucile Packard Foundation. T.P.R. and P.M. acknowledge the support of the U.S. Department of Energy, Office of Basic Energy Sciences, under contract FG03-88ER-45375.

12 March 1996; accepted 11 June 1996

Biomembrane Templates for Nanoscale Conduits and Networks

Evan Evans, Howard Bowman, Andrew Leung, David Needham, David Tirrell

Long nanotubes of fluid-lipid bilayers can be used to create templates for photochemical polymerization into solid-phase conduits and networks. Each nanotube is pulled from a micropipette-held feeder vesicle by mechanical retraction of the vesicle after molecular bonding to a rigid substrate. The caliber of the tube is controlled precisely in a range from 20 to 200 nanometers merely by setting the suction pressure in the micropipette. Branched conduits can be formed by coalescing separate nanotubes drawn serially from the feeder vesicle surface. Single nanotubes and nanotube junctions can be linked together between bonding sites on a surface to create a functionalized network. After assembly, the templates can be stabilized by photoinitiated radical cross-linking of macromonomers contained in the aqueous solution confined by the lipid bilayer boundary.

Recent developments in the fabrication of meso- and nanoscale structures have included the self-assembly of carbon and other materials into nanotubes and quantum wires (*1*) and the coalescence of lipid surfactants from solution into submicrometer tubules (*2*). Because of the bulk nature of the processes used to assemble such aggregates, it is difficult to preset the dimensions (such as tube length and the number of layers in the tube wall), and it is even more difficult to pattern macroscopic arrangements of the tube structures. New insights into the mechanics of biomembranes (*3*) led us to develop a simple method for the production of near-millimeter lengths of nanotubes, with calibers set by manual control (to an accuracy of ±10%) in the range of 20 to 200 nm. These tubes can be joined to form branched conduits and complex networks. Because these designs are made possible by the fluid property of the biomembrane interface, the challenge has been to develop chemical strategies to stabilize the membrane templates after patterning. Here, we introduce a method for the layout of nanotube networks and a photochemical polymerization process for stabilization of the resulting patterns in situ.

The formation of bilayer nanotubes from membrane capsules is a common occurrence in cell biology. For example, when a cell or vesicle sticks to a foreign surface at a point and is then pulled away, an optically invisible bilayer tube (diameter <100 nm) usually connects the capsule to the surface even after displacements of many diameters (*4*). Similarly, when vesicles are dehydrated to create large excesses of surface area or when cytoskeletal structures are destroyed inside cells, spherical blebs appear and remain tethered to the outer membrane by invisible bilayer tubes (*5*). The frequent occurrence of tethers shows that the closed spherical topology preferred by lamellar-phase lipids is extremely difficult to disrupt.

Two physical conditions are required for nanotube formation from bilayer vesicles: (i) the bilayer must be bonded to a spot on a rigid surface, and (ii) there must be a reservoir of excess bilayer surface, beyond that sufficient to enclose the vesicle volume as a sphere. These two conditions are easily attained and manipulated externally. First, vesicles after preparation (*6*) are slightly dehydrated by increasing the osmotic strength of the aqueous suspension. After aspiration into a micropipette, the excess surface of the vesicle is drawn into a projection inside the pipette (Fig. 1A), which

E. Evans and A. Leung, Departments of Physics and Pathology, University of British Columbia, Vancouver, British Columbia, Canada V6T 1W5.
H. Bowman and D. Tirrell, Polymer Science and Engineering Department, University of Massachusetts, Amherst, MA 01003, USA.
D. Needham, Department of Mechanical Engineering and Materials Science, Duke University, Durham, NC 27708, USA.

provides the reservoir of bilayer for nanotube production. If a few specialized lipids are mixed into the bilayer during preparation, strong point attachments are made when the vesicle is touched to a surface decorated with adhesive ligands (*7*) specific to the head groups of these lipids. When the pipette holding the vesicle is withdrawn, a nanotube is formed (Fig. 1, A and B). Both bright-field and fluorescence optical images show the feeder vesicle connected by the invisible nanotube to an immobilized microsphere coated with adhesive ligands. The nanotube is exposed by excitation of fluorescently labeled lipids doped in the bilayer surface. [The tube appears thick (~0.5 μm) in the fluorescence image because of optical diffraction. The actual dimension is an order of magnitude smaller (~40 nm).] Throughout the process, pipette suction P sets the level of tension T_m in the vesicle bilayer, that is,

$$T_m \approx \frac{PR_p}{2(1 - R_p/R)} \quad (1)$$

where R_p and R are the radii of the pipette lumen and the spherical body of the vesicle, respectively. In turn, the tension controls the nanotube diameter ($2r_t$), as established by a mechanical force balance (*3*), that is

$$r_t^2 = \frac{k_c}{2} T_m \quad (2)$$

where k_c is the bending stiffness of the bilayer (~10^{-19} N·m). Because of mass conservation, the rate of decrease in the projection length L_p inside the pipette as the nanotube length L_t is increased provides a macroscopic measurement of the invisible nanotube diameter, that is, the radius

$$r_t \approx -R_p \frac{dL_p}{dL_t} \quad (3)$$

(*3*, *4*). Nanotube diameter is controlled by bilayer tension (Fig. 2). This response is independent of the rate of tube extraction, which verifies that the mechanical force balance is dominated by the elastic properties of the bilayer (*3*). Finally, because the lipids are selected to form a fluid surface, two or more nanotubes drawn from the same feeder vesicle coalesce to a single junction when the vesicle is pulled away from the attachment sites. Fluorescence microscope images of the production process for a Y-branched nanotube element are shown in Fig. 3, A and B. Serial repetition of these procedures between points in an array of sites can create a complex network of nanotubes and branched elements.

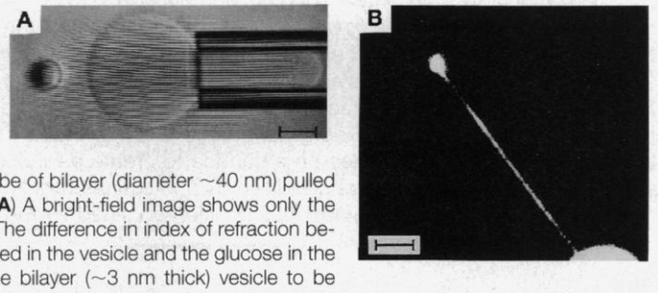

Fig. 1. Video microscope images of a lipid bilayer vesicle (diameter ~20 μm) held by micropipette suction and tethered to a solid microsphere (diameter ~4 μm) by an invisible nanotube of bilayer (diameter ~40 nm) pulled from the vesicle surface. (**A**) A bright-field image shows only the vesicle and microsphere. The difference in index of refraction between the sucrose contained in the vesicle and the glucose in the exterior solution allows the bilayer (~3 nm thick) vesicle to be observed clearly with Hoffman modulation contrast optics. (**B**) Epiillumination is used to excite fluorescence from labeled lipids doped in the bilayer, revealing the bilayer tube (diameter 40 nm) emanating from the vesicle. The vesicle was withdrawn from adhesive contact with the microsphere to produce the 50-μm-long tube. The cross section of the bilayer tube (which remains continuous with the vesicle surface) is an order of magnitude smaller than the apparent diffraction-limited thickness seen in the fluorescence image. Scale bars, 10 μm.

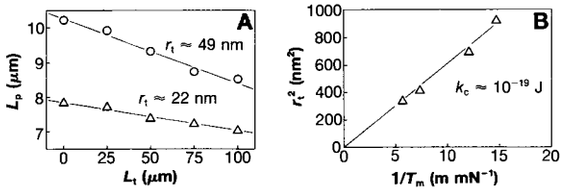

Fig. 2. Control of nanotube diameter by pipette suction applied to a bilayer vesicle made from pure stearoyl-oleoyl phosphatidylcholine. (**A**) Plots of vesicle projection length L_p inside the pipette versus nanotube length L_t as the vesicle was retracted from the adhesive surface at two levels of bilayer tension (set by pipette suction pressure). The slope of each plot yields the mean nanotube radius r_t. (**B**) Values of the square of the nanotube radius are plotted as a function of bilayer tension. The proportionality between the square of the tube radius and the reciprocal tension is one-half the bending or curvature elastic modulus of the bilayer, which yields $k_c = 10^{-19}$ J.

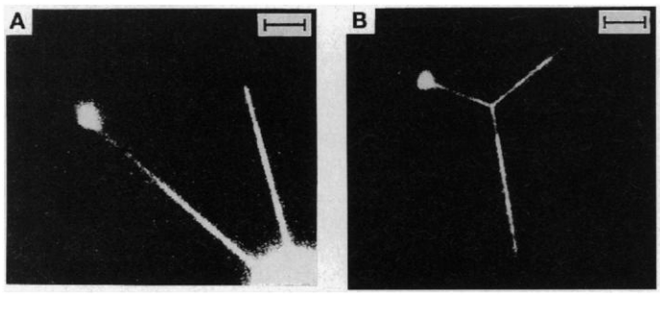

Fig. 3. Fluorescence microscope images of the manipulation sequence used to create a confluent junction of nanotubes (diameter ~40 nm). (**A**) First, two or more nanotubes are drawn successively from separate regions of the feeder vesicle surface. (**B**) Next, the vesicle is pulled away and the bilayer tubes slide over the fluid surface to coalesce at a perfect triangular junction, which implies that all three segments have the same bilayer tension and cross-sectional dimension. The procedure can be repeated to create an array of nanotube junctions. Scale bars, 10 μm.

Photoinitiated radical cross-linking of polyethylene glycol 1000 dimethacrylate (PEGDMA) was chosen as a prototype chemistry for stabilization of lipid bilayer templates. Cross-linked multimethacrylates form elastic networks that are widely used in applications where strength and shape stability are required (*8*). Of particular benefit, PEGDMA is soluble and swellable in both water and inorganic solvents, but after cross-linking the polymerized material forms a resilient and insoluble polyethylene glycol (PEG) gel. The PEG structure is attractive in the present context for several reasons: (i) The capability of swelling in aqueous and organic environments makes possible postpolymerization processing of patterns and networks in polar and nonpolar solvents. (ii) The PEG material does not denature enzymes or other proteins of potential interest in biosensor or biomaterials technology [PEG-modified enzymes are now being used in clinical applications (*9*)]. (iii) Likewise, PEG surfaces are relatively inert with respect to biological cells, which suggests that cell viability and function should not be altered in cellular devices that are composed of patterned PEGDMA networks. In our process, PEGDMA is present in the aqueous solution confined by the lipid bilayer and is cross-linked through radicals generated by dye-sensitized photooxidation of triethanolamine (*10*). Rose bengal is included as a photosensitizer for excitation by the 514-nm line of an argon ion laser (*11*).

Stable casts of lipid bilayer templates are shown in Fig. 4. The images show a variety

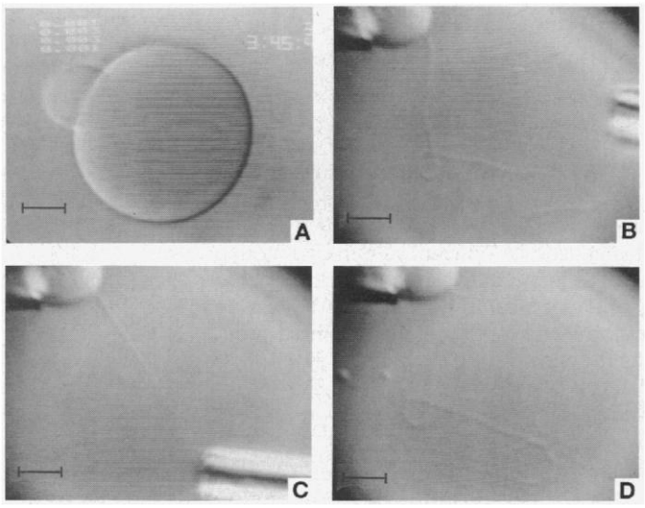

Fig. 4. Bright-field video images of rigid casts of vesicle and tube shapes after photopolymerization and detergent removal of the lipid bilayer template. The template was removed by addition of a quantity of sodium dodecyl sulfate sufficient to rupture bilayer vesicles that were not subjected to photopolymerization. (**A**) The cross-linked PEGDMA replica of a bilayer vesicle (diameter ~20 μm) aspirated initially into a micropipette. (**B**) The cross-linked PEGDMA core of a large bilayer tube (diameter ~0.5 to 1.0 μm) connected to the polymerized feeder vesicle. (**C**) A small-bore pipette pulls on the polymerized cylinder to demonstrate its mechanical strength. (**D**) After release, the tube relaxes and coils loosely like a flexible "rope." Scale bars, 10 μm.

of microscopic shapes after photopolymerization and removal of the lipid bilayer template by a detergent solution. In Fig. 4A, a vesicle (diameter ~20 μm) was cross-linked into a rigid replica of its smooth shape while held by micropipette suction. The images in Fig. 4, B to D, show a large tube (diameter ~0.5 to 1.0 μm) attached to the feeder vesicle after the cross-linking of the core and the removal of the bilayer. We found that the long cylinder could be repeatedly stressed by pulling on it with a small-bore micropipette (Fig. 4C). After each release, the cylinder merely relaxed into a loosely coiled "rope-like" shape (Fig. 4D). These results demonstrated the rigidity and flexibility of the cross-linked polymer structure. By comparison, fluid bilayer tubes are simply drawn back into the vesicle body by membrane tension unless restrained by a pulling force (Fig. 1B).

The techniques described above provide a basis for the fabrication of functional nanoscale conduit patterns and networks of various kinds. Lipid tubules can be used as precursors for the formation of submicrometer silica tubes (*12*) and as templates for the deposition of metals (*2*) and metal oxides (*13*); the methods developed in these earlier approaches should be directly applicable to the patterns described here and should produce robust structures with useful mechanical and electronic properties. The porous core of a polymerized nanotube provides unrestricted opportunity for the elaboration of network properties. Our results suggest that photo–cross-linking of water-soluble conjugated polymers can be used to produce networks of organic conductors and that impregnation of the core with metal salts can be used to metallize the structure after reduction. A similar approach for the deposition of metals in carbon nanotubes has been demonstrated (*14*). Moreover, the cross-linked core of nanotubes can also serve to immobilize enzymes or other proteins that are capable of modulating electron transfer or biochemical recognition processes. Finally, nanotube arrays can be used to extend recent advances in biosurface design (*15*) by linking patterns of biological cells immobilized on substrates to create integrated "cellular" biosensors and devices.

REFERENCES AND NOTES

1. S. Iijima, *Nature* **354**, 56 (1991); J. R. Heath and F. K. LeGoues, *Chem. Phys. Lett.* **208**, 263 (1993); N. G. Chopra *et al.*, *Science* **269**, 966 (1995).
2. J. M. Schnur, *Science* **262**, 1669 (1993).
3. E. Evans and A. Yeung, *Chem. Phys. Lipids* **73**, 39 (1994); A. Yeung, thesis, University of British Columbia (1994).
4. R. M. Hochmuth and E. A. Evans, *Biophys. J.* **39**, 71 (1982); _____, H. C. Wiles, J. T. McCown, *Science* **220**, 101 (1983); L. Bo and R. E. Waugh, *Biophys. J.* **55**, 509 (1989).
5. E. Evans and W. Rawicz, *Phys. Rev. Lett.* **64**, 2094 (1990).
6. We prepared giant bilayer vesicles (20 to 40 μm) by a method similar to previously published methods [D. Needham and E. Evans, *Biochemistry* **27**, 8261 (1988); D. Needham, *Methods Enzymol.* **220**, 111 (1993)]. The lipid composition was a mixture of 66 mol% stearoyl-oleoyl phosphatidylcholine, 33 mol% cholesterol (Avanti Polar Lipids, Alabaster, AL), and 1 mol% *N*-([6-(biotinoyl)amino]hexanoyl)-1,2-dihexadecanoyl-*sn*-glycero-3-phosphoethanolamine, triethylammonium salt (biotin-X-DHPE; Molecular Probes, Eugene, OR), in which biotin is conjugated to the DHPE lipid head group through a hydrocarbon spacer 10 to 15 Å long. The lipids were made up initially in chloroform-methanol (2:1) and spread on a Teflon disk. After evaporation of the volatile solvent for at least 6 hours in vacuum and constant darkness, the lipid paste was hydrated by a warm water–saturated argon jet for 15 min. Then the solution to be encapsulated (200 mM sucrose plus ingredients for polymerization) was gently added to the lipid multilayers. After the system was left to swell overnight, a sample of vesicles was harvested from the top of the beaker and resuspended in an equiosmolar glucose solution. In preparation for nanotube extrusion and photo–cross-linking, a small amount of the vesicle suspension was injected into a microchamber on the stage of an interference contrast videomicroscope. The glucose-sucrose differential ensured that the vesicles would sink to the bottom of the microscope chamber. For each test, a single vesicle was selected by micropipette and transferred into an adjacent test chamber, which contained avidin-coated microspheres as adhesive substrates for attachment to the vesicle surface. Details of the buffer solutions are described below.
7. The molecular attachment system chosen for these tests was the bacterial adhesion complex biotin-avidin. As noted above, the vesicle bilayer was doped with a small concentration of biotinylated lipids so that, when touched to a substrate decorated with avidin, the bilayer would bond strongly to the surface. The attachment substrates were silica or glass microspheres that we prepared by adding ~10^5 spheres to 1 ml of a solution (50 μg ml^{-1}) of Avidin NeutraliteT (Molecular Probes) in 150 mM NaCl. The avidin physiosorbed strongly to the bead surfaces. To prepare a pattern of sites for network formation, we coated the glass floor of the microchamber with a monolayer of biotinylated serum albumin; then the avidin-coated microspheres were positioned on the surface and immobilized by adhesive bonds. The avidin-biotin system was chosen only as a prototype to demonstrate attachments to solid surfaces. For microdevices, a more appropriate method would be to use thiol groups for bonding to gold or silver contacts (*15*). The thiol sulfur atoms form covalent bonds to these metal substrates. As such, thiol-conjugated amphiphiles could be synthesized and incorporated into the lipid bilayer of the vesicle to permit attachments to gold regions on a microchip surface.
8. K. S. Anseth, L. M. Kline, T. A. Walker, K. J. Anderson, C. N. Bowman, *Macromolecules* **28**, 2491 (1995).
9. M. S. Hershfield *et al.*, *N. Engl. J. Med.* **316**, 589 (1987).
10. D. F. Eaton, *Adv. Photochem.* **13**, 427 (1986); A. Zakrzewski and D. C. Neckers, *Tetrahedron* **43**, 4507 (1987).
11. Vesicles were formed in a solution containing 200 mM sucrose, 100 mM triethanolamine, 0.1 mM rose bengal, and 10 weight % PEGDMA. After resuspension in equiosmolar glucose solution and injection into the microscope chamber, a single vesicle was transferred into an adjacent microchamber containing a slightly hyperosmotic glucose solution plus 0.1 mM rose bengal, 100 mM triethanolamine, 25 mM NaCl, 2 weight % PEG 2000 (no methacrylate groups), and 0.2 weight % albumin. After pattern formation, polymerization of the PEGDMA confined inside the lipid bilayer boundary was initiated by irradiation with the 514-nm line of a Coherent Inova 90-4 laser for ~2 min.
12. S. Baral and P. Schoen, *Chem. Mater.* **5**, 145 (1993).
13. D. D. Archibald and S. Mann, *Nature* **364**, 430 (1993).
14. S. C. Tsang, Y. K. Chen, P. J. F. Harris, M. L. H. Green, *ibid.* **372**, 159 (1994); R. M. Lago, S. C. Tsang, K. L. Lu, Y. K. Chen, M. L. H. Green, *J. Chem. Soc. Chem. Commun.* **1995**, 1355 (1995).
15. G. M. Whitesides, J. P. Mathias, C. T. Seto, *Science* **254**, 1312 (1991); G. M. Whitesides, *Sci. Am.* **273** (no. 3), 146 (1995).

16. This development was motivated by the Canadian Institute for Advanced Research Program in Science of Soft Surfaces and Interfaces. Additional support came from Canadian Medical Research Council grant MT 7477 (E.E.), the University of Massachusetts Materials Research Science and Engineering Center (D.T.), and North Carolina Biotechnology Center grant 9413 ARG-0018 (D.N. and E.E.).

4 March 1996; accepted 29 May 1996